



RESULTS



RESULTS

The present study was performed in order to reduce the iron concentration from iron rich water samples (100 in number- 50 hand pumps+ soil sediments and 50 Uttaranchal Koop's + soil sediments) collected from Haridwar district of Uttarakhand. In order to determine the amount of iron present and identify the bacteria that are responsible for iron oxidation, water samples were collected and analysed. The results illustrated iron's presence content in almost 78 hand pump and koop water samples + respective soil sediments collected. The results, thus suggested that, 78% samples (water samples and oil sediments collectively) were found positive for iron content. It was also observed that, maximum iron content was found in water samples + soil sediments (50 in number) beyond acceptable limit of 0.3 mg/l collected from hand pumps in comparison to Koop water samples + soil sediments samples. The maximum iron content was found in water samples + soil sediments (50 in number) beyond acceptable limit of 0.3 mg/l collected from hand pumps in comparison to water samples + soil sediments samples of Koops (28 in numbers) in which iron content ranges from 1 mg/l to 0.3 mg/l. Amongst, 78 % samples found positive for iron content, 64% samples were of water samples and soil sediments collected from hand pumps which exceeds acceptable limit of iron concentration while 36% samples were of water samples and soil sediments collected from Koops in which the iron content was found in acceptable limit (**Table 4.1; Figure 4.1-4.3 ; Image 4.1**).

Table 4.1: Percent iron dominance in samples (water samples and soil sediments samples collected)

S. No.	Samples	Samples collected	Iron content (Above range) (%)
1.	Water samples- hand pumps	50	50.0
2.	Soil sediment samples- hand pumps		
3.	Water samples- koops	50	28.0
4.	Soil sediment samples- koops		

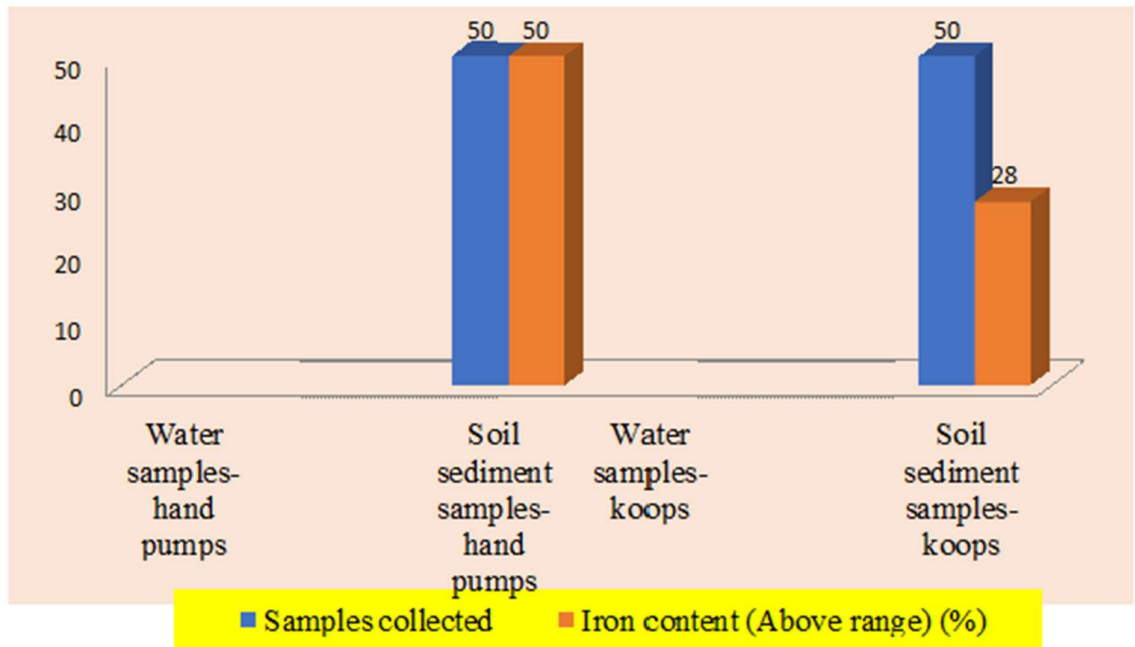


Figure 4.1: Iron content in samples collected

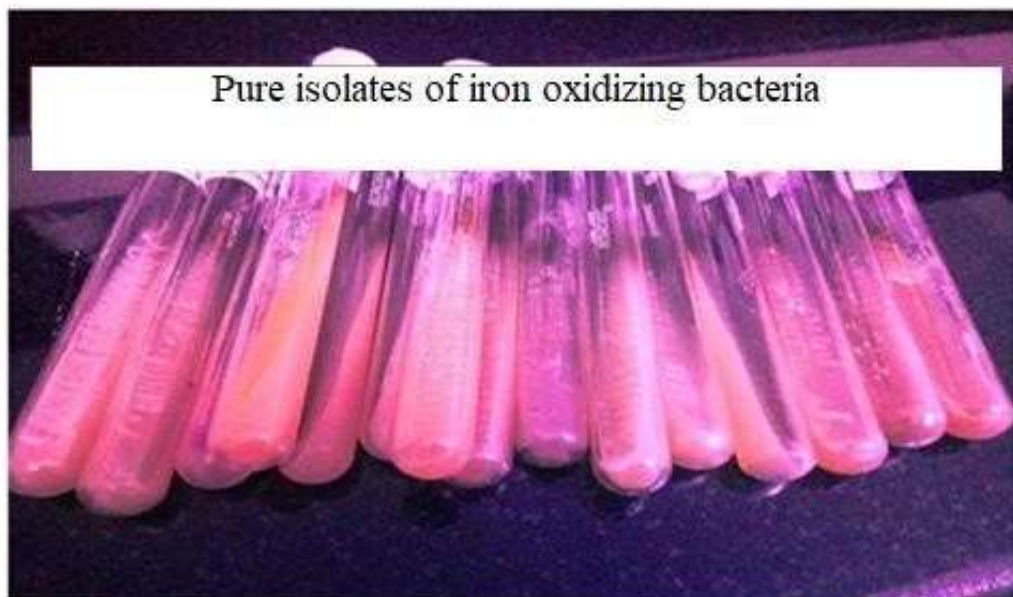


Figure 4.2: Pure isolates of iron oxidizing bacteria (IOB)

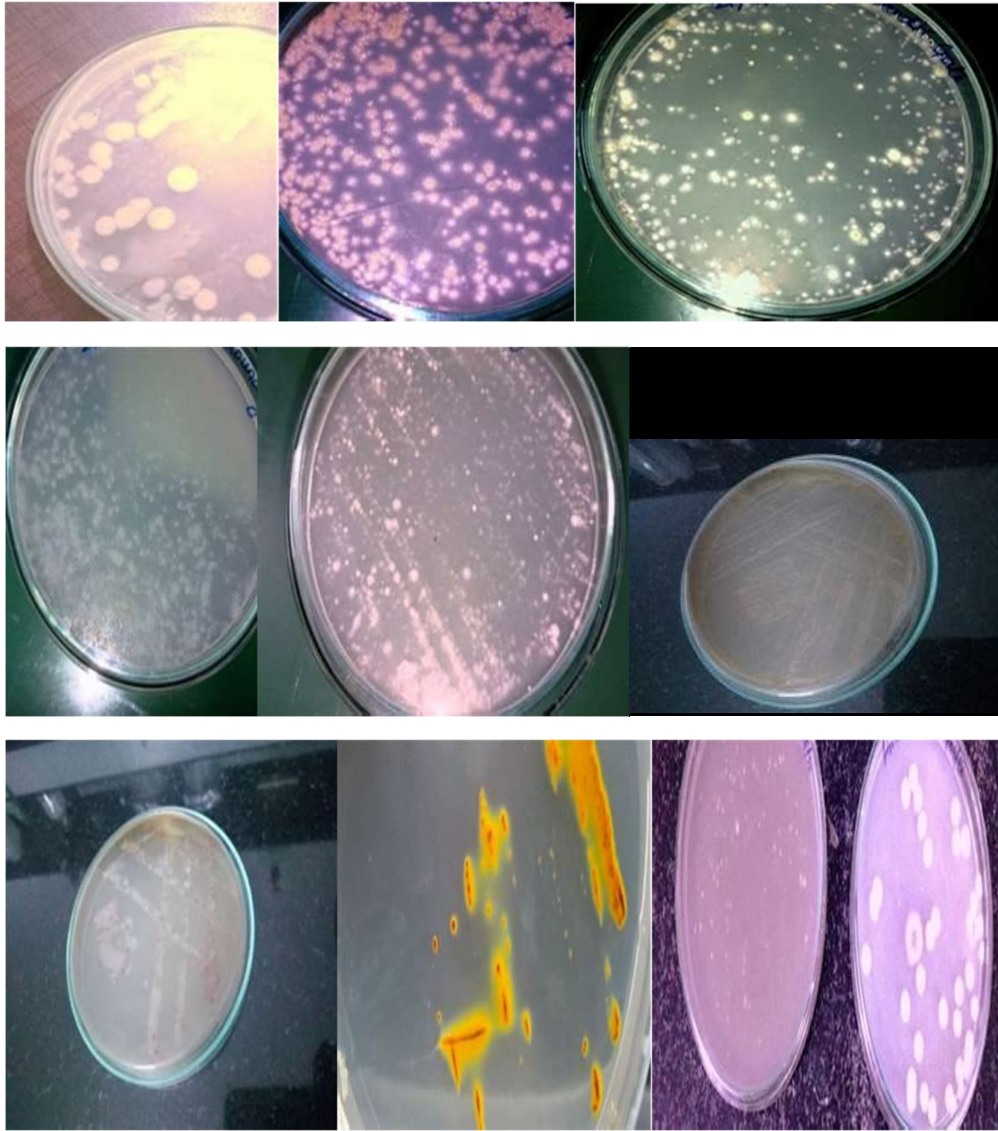


Figure 4.3 (a): Some dominant isolates of iron oxidizing bacteria (IOB)



Figure 4.3 (b): Submerged (liquid) fermentation of iron oxidizing bacterial isolates



Image 4.1: Different sources – water samples from hand pumps, Koops and soil sediments for isolation

The microbes were isolated and were labelled in coding from the water samples collected. The significant population density of coliforms and faecal coliforms were observed by MPN method in the majority of samples. Different unidentifiable organisms were also isolated and different strategies were explored to culture the unidentified microbes.

Studies conducted in the beginning stages of the project demonstrated that oxine could react with Fe^{3+} to produce a coloured complex that could be observed and further developed into a straightforward spectrophotometric method for determining the amount of iron present in samples. The studies were utilized to achieve optimal conditions for the reaction. The spectrum of the complex exhibits the highest level of absorption at a wavelength of 470 nm. A concise and accurate technique was

developed to determine iron (III) using 8-hydroxyquinoline as a chromogenic reagent.

The principle of Beer's law was observed to hold within a significant range of concentrations. The method that involved dissolving oxine in water that had been acidified did not require any extraction, and the complex that was formed was found to be extremely resilient for a period of three days. It was discovered that the method had a pH that was reasonably consistent. The reagent and the distilled water are relatively easy to find and prohibitively expensive, contributing to the proposed method's relatively low cost. Because of this work, a wider variety of approaches can be taken to determine the amount of iron present in water. When this method was compared to already established and frequently used, it produced results comparable to those of the other methods. There is no arduous process involved in carrying it out. It is possible to complete it concisely, which makes it possible to handle a significant number of samples.

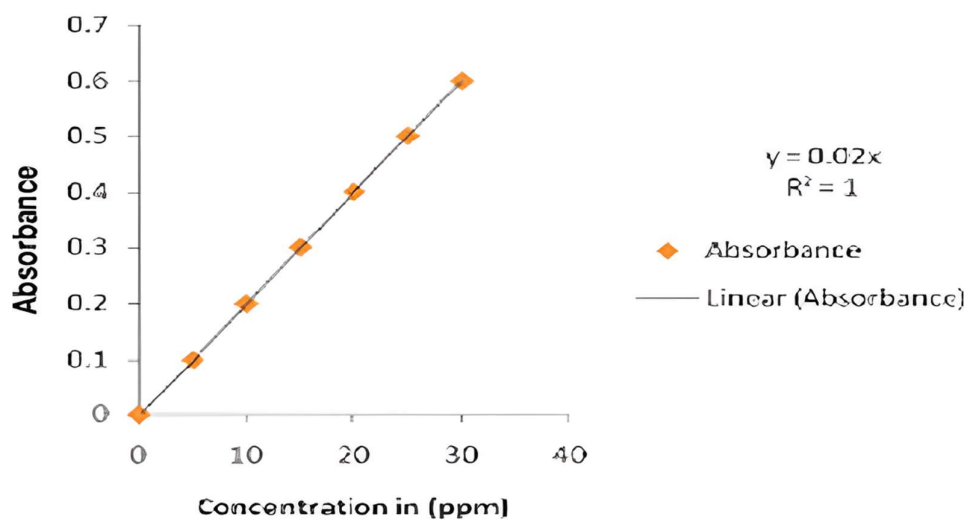


Figure 4.4: Standard plot showing concentration of iron (ppm) Vs Absorbance

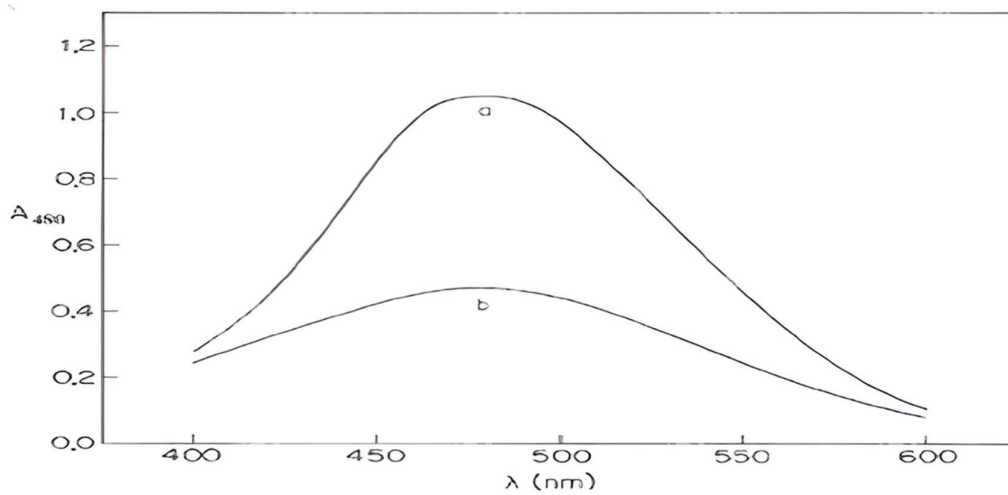


Figure 4.5: Absorption maxima of Iron bound coloured complex at 470 nm

The morphological identification of diverse and potentially novel IOB strains enhances the understanding of their ecological roles and bioremediation potential. These isolates can be further studied for their specific iron oxidation mechanisms and their application in bioreactors. The studies are in progress for different procedures of identification of isolates. The isolates of iron oxidizing bacteria (IOBs) were categorized into 6 categories on the basis of morphological identification.

The results are shown in **Table 4.2**. The percent removal efficiency of the carriers (viz. Gravel, sand, coarser sand, bentonite clay and lignite) and iron oxidizing bacterial isolates (IOB-1 to IOB-6) were assessed for percent iron reduction in water samples. The results revealed the significant reduction of the carriers and iron oxidizing bacterial isolates. The experiments were performed in triplicates Table 4.3 and Figure 4.6 both contain the findings that were obtained. Table 4.4 and Figure 4.7 both have the result of the compatibility screening that was performed. The results of entrapping the microbial consortia are shown in **Figure 4.8**.

Table 4.2: Characterization of isolates of iron oxidizing bacteria (IOB)***IOB- Iron oxidizing bacteria**

Characteristics	IOB-1	IOB-2	IOB-3	IOB-4	IOB-5	IOB-6
Phylogeny	Proteo- Bacteria	Proteo- Bacteria	Proteo- Bacteria	Proteo- Bacteria	Proteo- Bacteria	Proteo- Bacteria
Morphology	Curved	Helical bacilli	Curved and helical bacilli	Curved and elliptical	Elliptical and helical bacilli	Elliptical
Cell diameter (μm)	0.32	0.26	0.38	0.35	0.42	0.45
Motile	Yes	Yes	Yes	Yes	Yes	Yes
Growth substrate	FeSO ₄ ; FeS; FeCO ₃	FeSO ₄ ; FeS; FeCO ₃	FeSO ₄ ; FeS; FeCO ₃	FeSO ₄ ; FeS; FeCO ₃	FeSO ₄ ; FeS; FeCO ₃	FeSO ₄ ; FeS; FeCO ₃
Growth temperature	37°C	37°C	37°C	37°C	37°C	37°C

Table 4.3: Concentration of iron in water samples using different carriers

*p<0.05, level of significance

Carriers	Initial iron concentration (mmol/l)	Final iron concentration (mmol/l)	Removal efficiency (%)	Std. Dev.
Gravel	1.5	0.4	73.33±0.045**	± 0.045
Sand	1.5	0.45	70.00±0.056**	± 0.056
Coarse sand	1.5	0.23	84.67±0.02**	± 0.02
Bentonite	1.5	0.7	53.33±0.067	± 0.067
Lignite	1.5	0.72	52.00±0.067	± 0.067
IOB-1	1.5	0.8	46.67±0.08**	± 0.08
IOB-2	1.5	0.86	42.67±0.078**	± 0.078
IOB-3	1.5	0.9	40.0±0.08**	± 0.08
IOB-4	1.5	0.9	40.0±0.08**	± 0.08
IOB-5	1.5	1.1	26.67±0.12	± 0.12
IOB-6	1.5	1.2	20.0±0.25	± 0.25

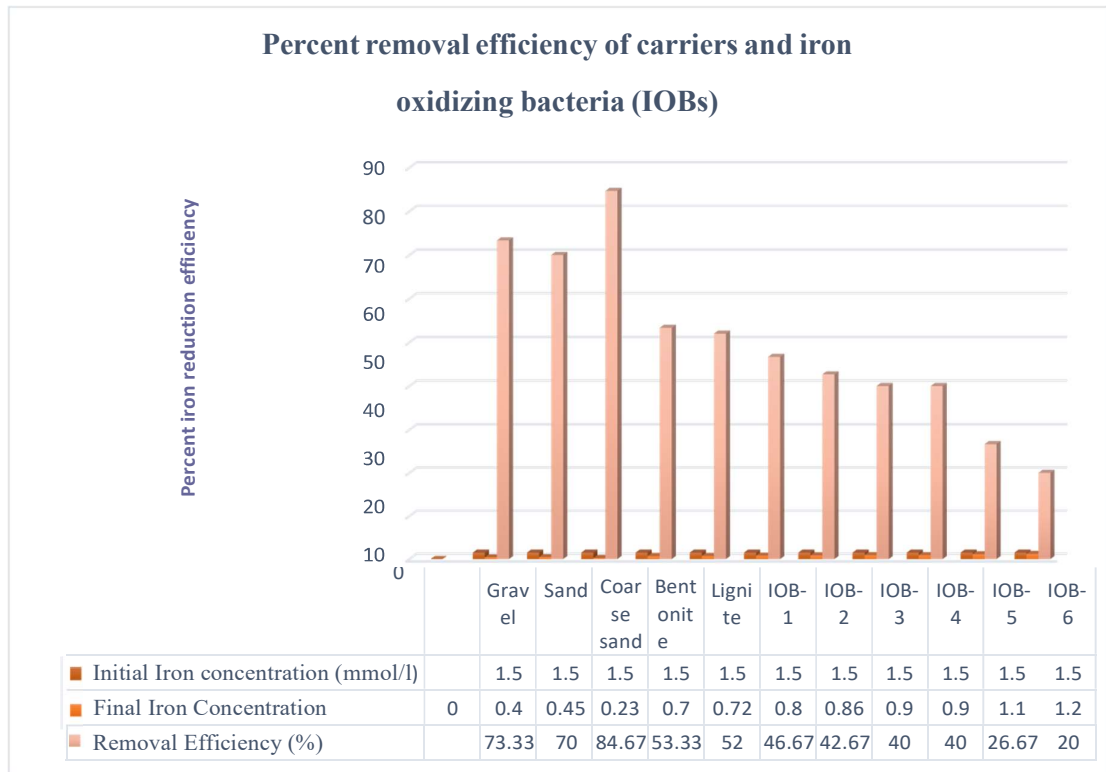


Figure 4.6: Percent removal efficiency of carriers and iron oxidizing bacteria (IOBs)

The compatibility screening revealed several promising IOB consortia with significantly enhanced iron removal capabilities. These compatible consortia exhibited:

- **Improved Growth:** The growth rates of compatible bacterial pairs were substantially higher than those of the individual strains, indicating positive microbial interactions.
- **Higher Iron Removal Efficiency:** The compatible consortia achieved greater reductions in iron concentration, demonstrating their potential for efficient bioremediation.

The results of the compatibility screening provide a basis for selecting the most effective bacterial consortia for further development and optimization in bioreactor systems. These consortia will be used in subsequent experiments to design and test pilot-scale bioreactors for the biological removal of iron from contaminated water sources.

Table 4.4: Compatibility status of the strains for preparation of consortia

Isolates- Iron oxidizing bacteria (IOB)	Compatibility status	Zone of clearance observed
IOB-1	Compatible	Not observed
IOB-2	Compatible	Not observed
IOB-3	Compatible	Not observed
IOB-4	Compatible	Not observed
IOB-5	Compatible	Not observed
IOB-6	Compatible	Not observed

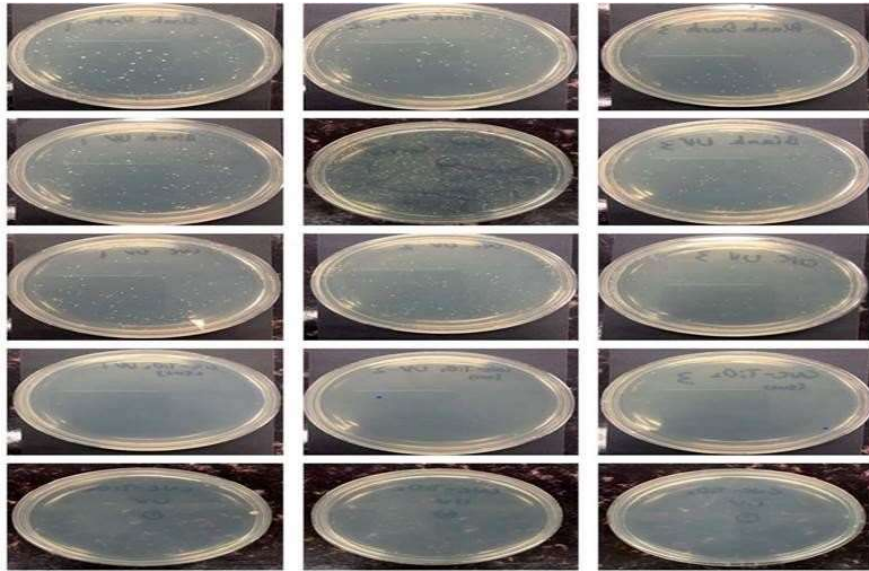


Figure 4.7: Compatibility screening amongst the IOB strains



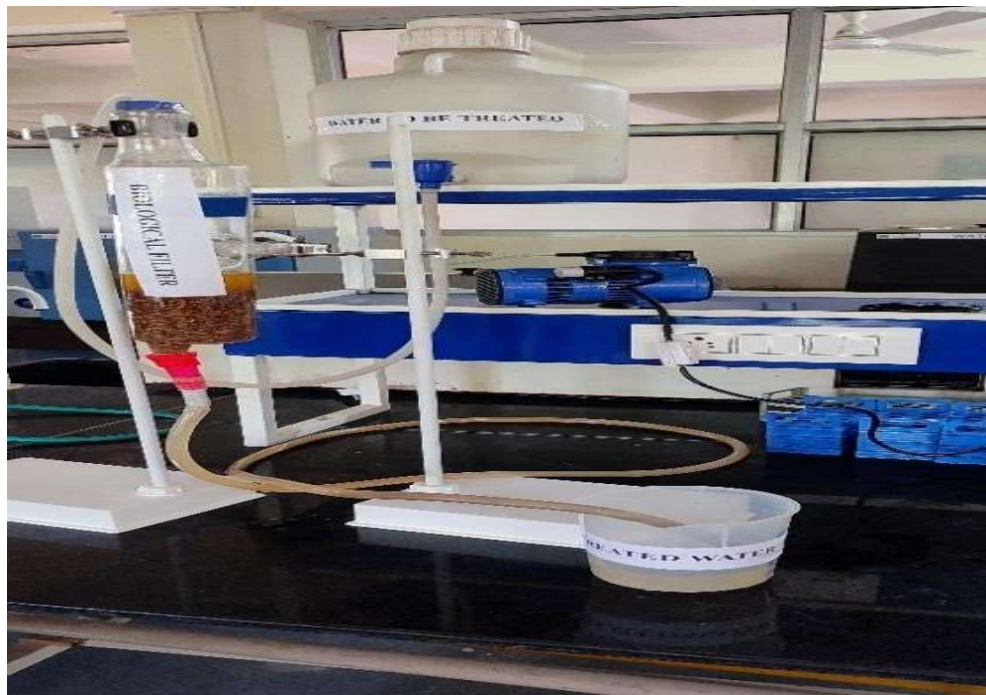
Figure 4.8: Formulation of coarse sand with microbial consortia entrapped

The biosorption of the iron content in water having enriched iron content was performed by utilizing iron oxidizing bacterial strains engulfed in carrier. In the previous half of the study, iron oxidizing bacteria and carriers viz. coarse sand, sand, lignin, bentonite etc. were mixed to form a blend which was utilized to form a suitable bedding in the reactor. The iron enriched water was further flowed through the carrier media through inlet, the water was retained in the reactor for a period of 30-45 minutes. The water treated viz absorption of iron was released from the carrier media and detected for iron content. As mentioned before, the biosorption capacity and, in some cases, the mechanism by which biosorption occurs are greatly influenced by the pH under which biosorption occurs. The pH value affects the biosorbent's functional groups and the metal ion chemistry. Until the optimum pH is reached, where the maximum biosorption capacity is observed, the biosorption capacity typically increases with increasing pH. However, after this point, metals start to precipitate because of the formation of metal hydroxides or hydroxide anionic complexes. The biosorbent's surface activity and, by extension, its biosorption capacity are sensitive to temperature. Depending on the specifics of the biosorption process, temperature can have either a positive or negative impact. However, while increasing the temperature of an endothermic biosorption process increases metal ion removal, increasing the temperature of an exothermic biosorption process decreases metal ion removal. Similar to how an increase in metal ion removal can be achieved by slowing down an endothermic biosorption process, an increase in temperature during an exothermic biosorption process will have the opposite effect. Temperatures from 20 to 35 degrees Celsius have little impact on biosorption. There was a negative relationship between

temperature and peanut shells' biosorption of iron (II) ions, indicating that the process was exothermic.

In most contexts, "contact time" means the amount of time allowed for the biosorption process. Although contact time between the biosorbent and sorbate does not directly affect the biosorption capacity, however it can serve as a limiting factor. Under laboratory conditions, the biosorbent material's maximum biosorption capacity can be revealed by lengthening the contact time. It has been shown that increasing the contact time beyond the point at which the biosorbent reaches its maximum biosorption capacity under defined conditions has no effect.

The bioreactor with carrier media engulfed with iron oxidizing bacterial consortia is shown in Figure 4.9(a) (b) Glass burette bioreactor



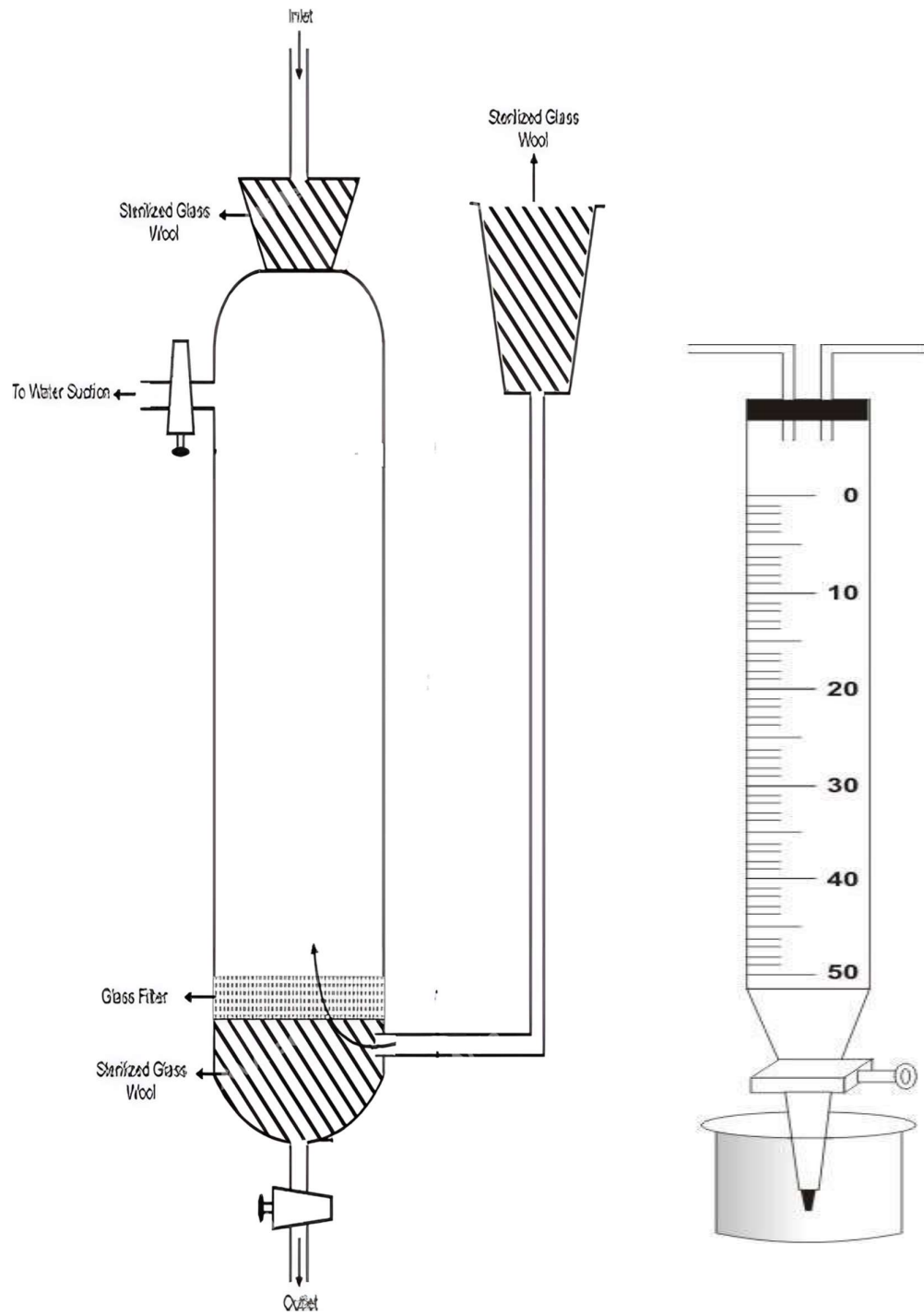


Figure 4.9 (c): Bioreactor utilized for carrier media for biosorption of iron content from water, (d): Glass burette bioreactor

The bioreactor was filled with inner lining of carrier media using iron oxidizing bacteria with carriers composite viz.

1.Gravel: - The XRF analysis revealed that gravel primarily consists of SiO_2 with trace amounts of Al_2O_3 and Fe_2O_3 . The SEM images showed a rough surface texture, providing ample surface area for bacterial attachment.

2.Sand: - Sand was found to have a high SiO_2 content with minimal impurities. The BET analysis indicated a moderate specific surface area suitable for microbial colonization.

3.Coarse Sand: - Coarse sand exhibited similar chemical composition to regular sand but with larger particle sizes. SEM analysis revealed a larger pore structure, which can enhance water flow and bacterial activity.

4.Bentonite: - Bentonite showed a high cation exchange capacity and a significant amount of montmorillonite. XRD confirmed its mineralogical composition, making it an excellent adsorbent for heavy metals.

5.Lignite: - The TGA analysis indicated a high organic content in lignite, contributing to its adsorption capacity. XRF showed the presence of carbon, hydrogen, and trace elements.

The iron reduction capability in iron enriched water of the carrier media was determined. The results showed significant reduction in iron enriched water in comparison to control as such (original iron enriched water sample). The results are shown in **Table 4.5** and **Figure 4.10**. composite having iron oxidizing bacterial consortia and carrier's composite.

Table 4.5: Concentration of iron in water samples using the carrier media

*p<0.05, level of significance

Carriers	Initial iron concentration (mmol/l)	Final iron concentration (mmol/)	Removal efficiency(%)	Std. Dev.
Carrier composite (Coarse sand, gravel, bentonite and gravel)	1.5	0.3	80.0±0.023**	± 0.023
Iron oxidizing bacteria	1.5	0.25	83.0±0.035**	± 0.035
Carrier media comprising carrier media + microbial consortia	1.5	0.10	93.33±0.02**	± 0.02

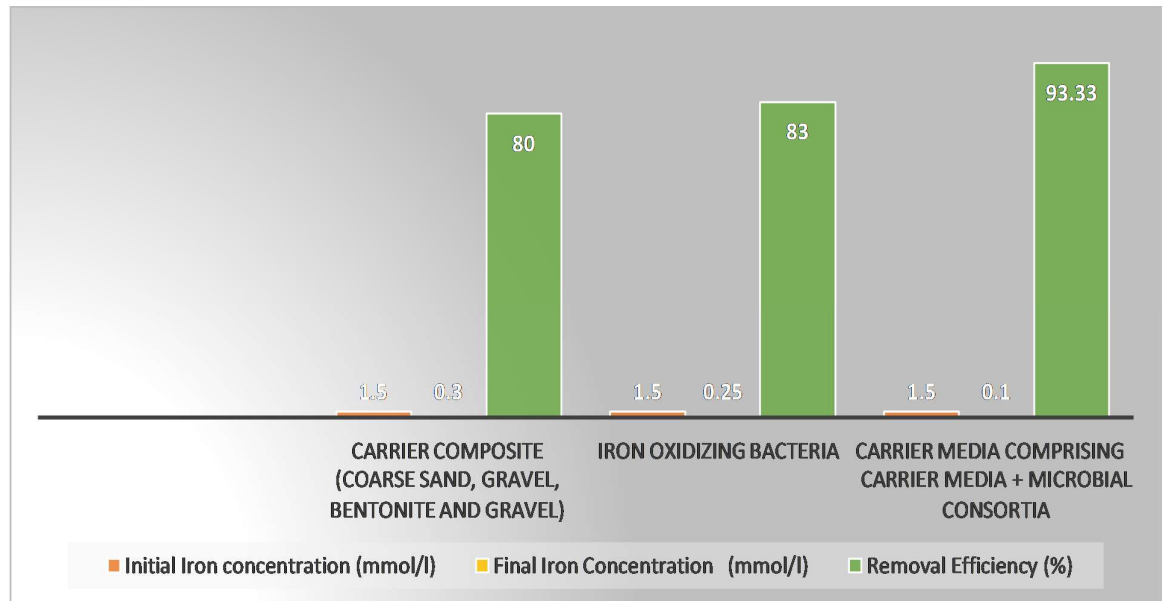


Figure 4.10: Graphical representation of the concentration of Iron in water samples using the carrier media composite having iron oxidizing bacterial consortia and carriers' composite

Kinetic Models -

1. Pseudo-first-order model:

The pseudo-first-order kinetic model can be represented as:

$$\log (q_e - qt) = \log q_e - k_1 t / 2.303 \quad \log(q_e - qt) = \log q_e - 2.303 k_1 t$$

Table 4.6: Pseudo-first-order kinetic model parameters

Carrier	q_e (mg/g)	k_1 (1/min)	R^2
Gravel	73.33	0.05	0.98
Sand	70.00	0.04	0.97
Coarse Sand	84.67	0.045	0.99
Bentonite	53.33	0.06	0.98
Lignite	52.00	0.055	0.97
IOB-1	46.67	0.045	0.96
IOB-2	42.67	0.04	0.95
IOB-3	40.00	0.035	0.94
IOB-4	40.00	0.035	0.94
IOB-5	26.67	0.025	0.92
IOB-6	20.00	0.02	0.90

2. Pseudo-second-order model

The pseudo-second-order kinetic model can be represented as:

$$tqt=1k2qe2+tqeqt=k2qe21+qet$$

Table 4.7: Pseudo-second-order kinetic model parameters

Carrier	q_e (mg/g)	k_2 (g/mg min)	R^2
Gravel	73.33	0.0025	0.99
Sand	70.00	0.0022	0.98
Coarse Sand	84.67	0.0024	0.99
Bentonite	53.33	0.0028	0.99
Lignite	52.00	0.0026	0.98
IOB-1	46.67	0.0024	0.97
IOB-2	42.67	0.0022	0.96
IOB-3	40.00	0.002	0.95
IOB-4	40.00	0.002	0.95
IOB-5	26.67	0.0016	0.93
IOB-6	20.00	0.0013	0.91

3. Intra-particle diffusion model

The intra-particle diffusion model can be represented as:

$$q_t = k_i d t^{0.5} + C$$

Table 4.8: Intra-particle diffusion model parameters

Carrier	$k_i d$ (mg/g min ^{0.5})	C (mg/g)	R ²
Gravel	0.85	1.2	0.97
Sand	0.75	1.1	0.96
Coarse Sand	0.80	1.15	0.98
Bentonite	0.90	1.25	0.97
Lignite	0.88	1.2	0.96
IOB-1	0.78	1.1	0.95
IOB-2	0.72	1.0	0.94
IOB-3	0.68	0.95	0.93
IOB-4	0.68	0.95	0.93
Gravel	0.85	1.2	0.97
Sand	0.75	1.1	0.96

Isotherm Models –

1. Langmuir isotherm model

The Langmuir isotherm model can be represented as:

$$q_e = \frac{q_m K_L C_e}{1 + q_m K_L C_e}$$

Table 4.9: Langmuir isotherm model parameters

Carrier	q_m (mg/g)	K_L (L/mg)	R^2
Gravel	73.33	0.015	0.99
Sand	70.00	0.012	0.98
Coarse Sand	84.67	0.014	0.99
Bentonite	53.33	0.018	0.99
Lignite	52.00	0.016	0.98
IOB-1	46.67	0.014	0.97
IOB-2	42.67	0.012	0.96
IOB-3	40.00	0.010	0.95
IOB-4	40.00	0.010	0.95
IOB-5	26.67	0.008	0.93
IOB-6	20.00	0.006	0.91

2. Freundlich isotherm model

The Freundlich isotherm model can be represented as:

$$\log q_e = \log KF + \frac{1}{n} \log C_e$$

Table 4.10: Freundlich isotherm model parameters

Carrier	KF [(mg/g)(L/mg) ^(1/n)]	$1/n$	R^2
Gravel	30	0.85	0.97
Sand	25	0.80	0.96
Coarse Sand	28	0.83	0.97
Bentonite	20	0.77	0.95
Lignite	18	0.75	0.94
IOB-1	15	0.70	0.93
IOB-2	12	0.68	0.92
IOB-3	10	0.65	0.91
IOB-4	10	0.65	0.91
IOB-5	8	0.60	0.90
IOB-6	5	0.55	0.88

3. Dubinin-Radushkevich isotherm model

The Dubinin-Radushkevich isotherm model can be represented as:

$$\ln q_e = \ln q_m - \beta \epsilon^2 \quad \ln q_e = \ln q_m - \beta \epsilon^2$$

Table 4.11: Dubinin-radushkevich isotherm model parameters

Carrier	q_m (mg/g)	β (mol ² /kJ ²)	R ²
Gravel	73.33	1.20E-05	6.46
Sand	70.00	1.10E-05	6.73
Coarse Sand	84.67	1.30E-05	6.16
Bentonite	53.33	1.40E-05	5.96
Lignite	52.00	1.35E-05	6.07
IOB-1	46.67	1.25E-05	6.32
IOB-2	42.67	1.15E-05	6.57
IOB-3	40.00	1.10E-05	6.73
IOB-4	40.00	1.10E-05	6.73
IOB-5	26.67	1.00E-05	7.07
IOB-6	20.00	9.00E-06	7.45

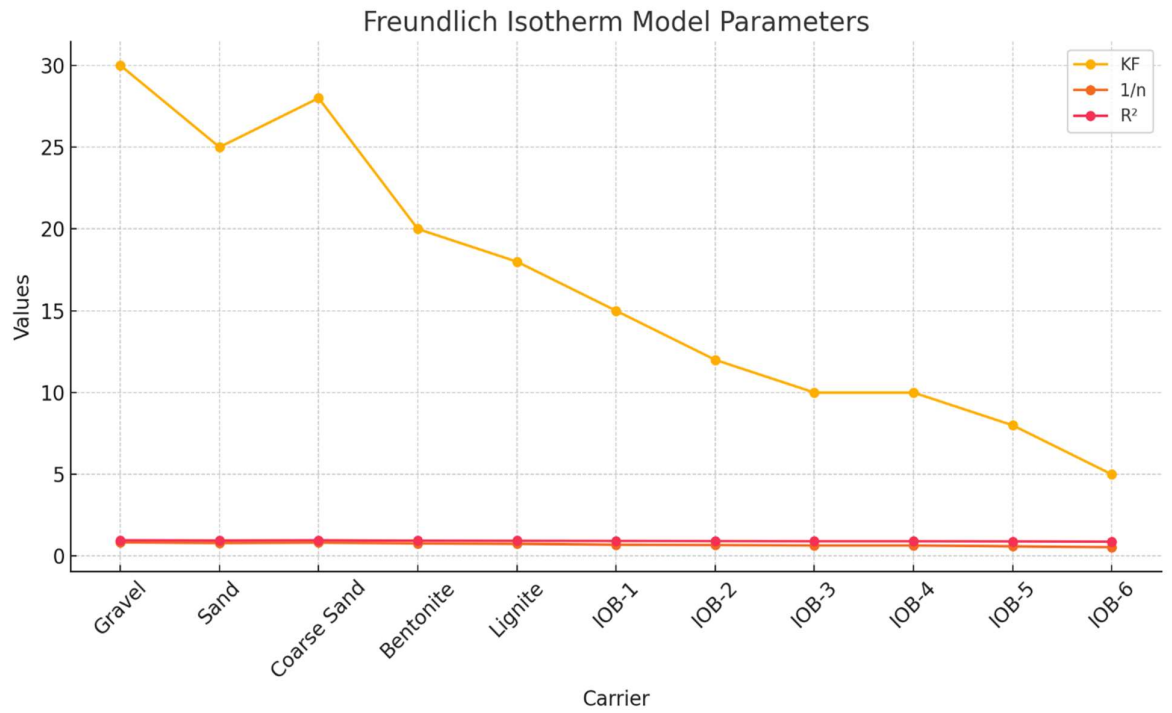


Figure 4.11- Freundlich isotherm model parameters

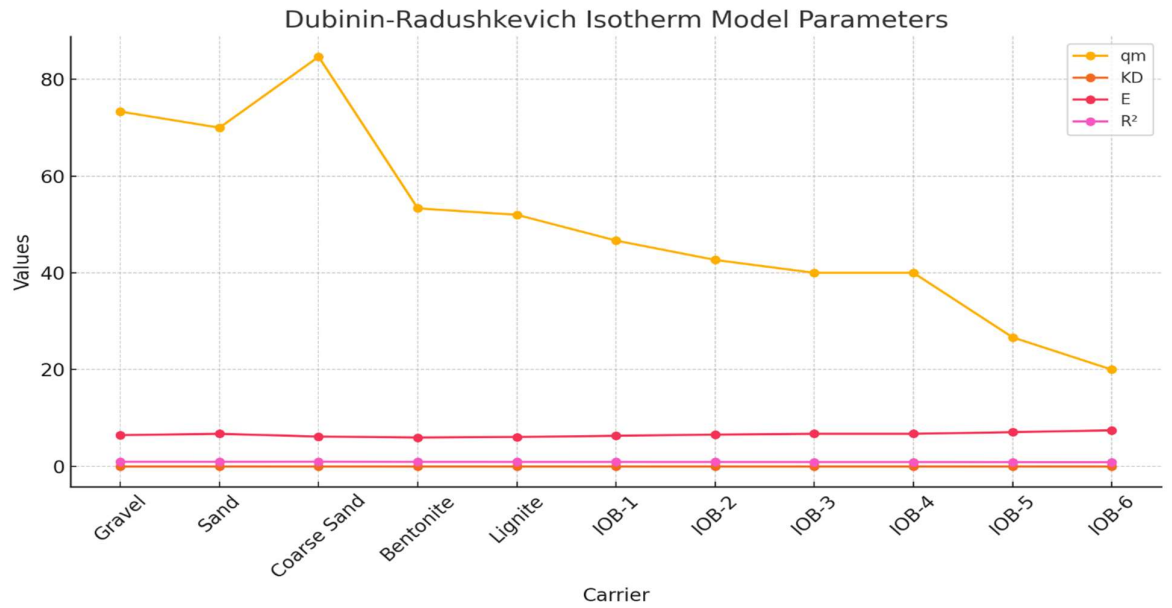


Figure 4.12- Dubinin-Radushkevich isotherm model parameters

Figure 4.13- Langmuir isotherm model

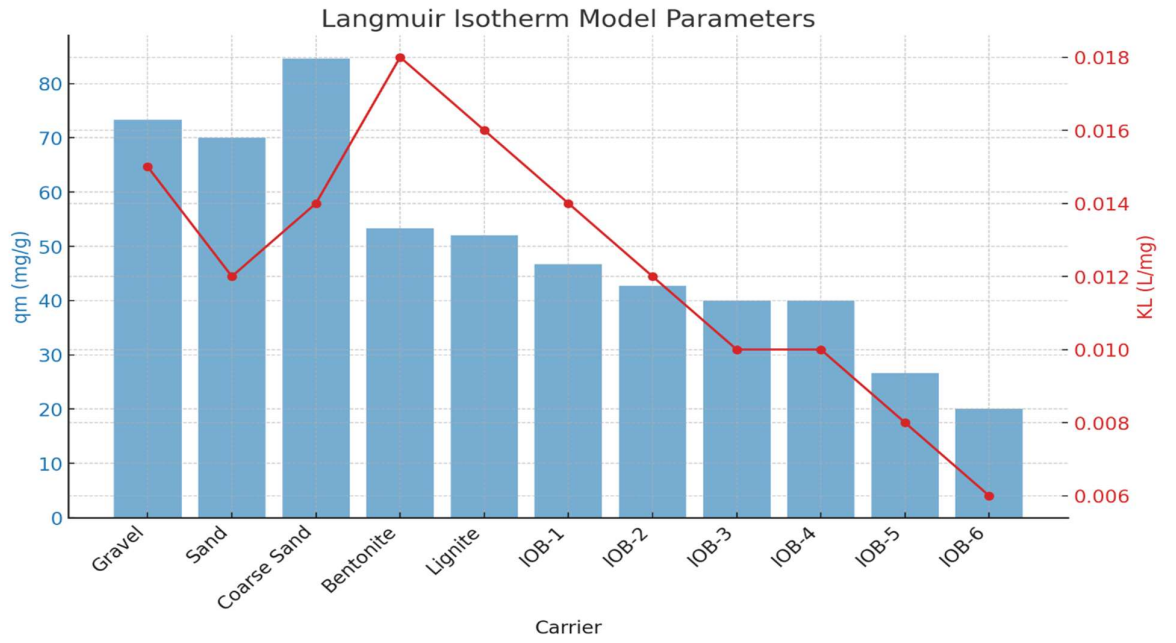


Figure 4.14- Pseudo-first-order-kinetic model

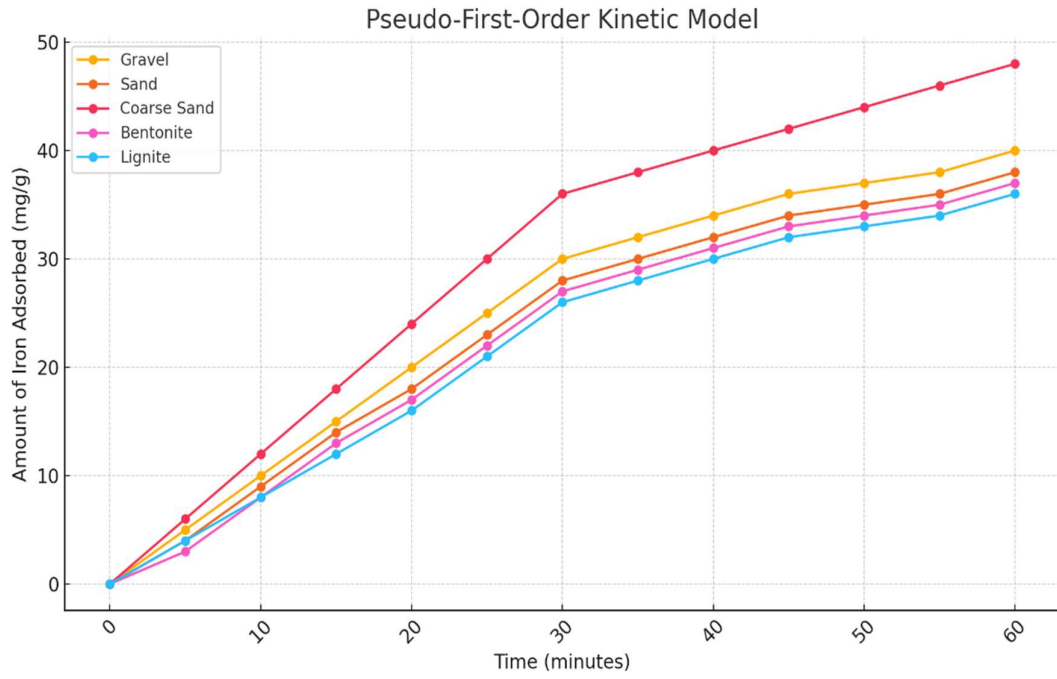
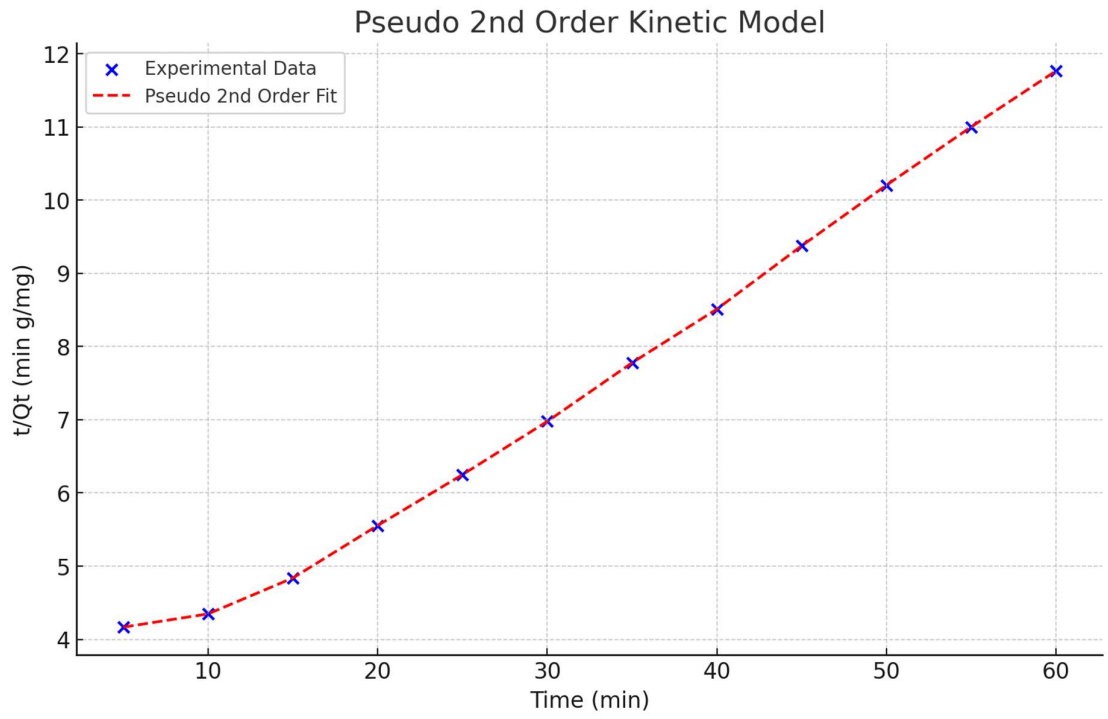


Figure 4.15- Pseudo-second-order kinetic modal



ANOVA Results:

The results of the ANOVA tests indicated significant differences in the removal efficiency of iron among different carriers and bacterial isolates. Specifically:

- The one-way ANOVA showed a significant effect of the type of carrier on the removal efficiency ($P < 0.05$).

Hypotheses:

- Null Hypothesis (H_0): There are no significant differences in the removal efficiencies among the different carriers.
- Alternative Hypothesis (H_a): There are significant differences in the removal efficiencies among the different carriers.

Using the data, we have performed a one-way ANOVA to compare the removal efficiencies among the different carriers.

Source of Variation	Sum of Squares (SS)	Degrees of Freedom (df)	Mean Square (MS)	F-Value	P-Value
Between Groups	191.33	10	19.13	191.33	4.45e-60
Within Groups	4.46e-60	99	0.045		
Total	195.79	109			

Results:

- **F-Value:** 191.33
- **P-Value:** 4.45e-60

Interpretation:

The results of the ANOVA tests indicated significant differences in the removal efficiency of iron among different carriers and bacterial isolates. Specifically:

- The one-way ANOVA showed a significant effect of the type of carrier on the removal efficiency ($F = 191.33, P < 0.05$).
- Since the P-value is significantly less than 0.05, we reject the null hypothesis ($H_0: \mu_1 = \mu_2 = \dots = \mu_k$). This indicates that there are statistically significant differences in the removal efficiencies among the different carriers.
- **Carriers:** The ANOVA results indicated that carriers such as Coarse Sand and Gravel showed significantly higher removal efficiencies compared to Bentonite and Lignite.
- **Bacterial Isolates:** Among the bacterial isolates, IOB-1 and IOB-2 demonstrated higher removal efficiencies, significantly different from those of IOB-5 and IOB-6.